Korean J. Chem. Eng., **25**(6), 1331-1337 (2008)

Synthesis, crystal structure and dehydration kinetics of $NaB(OH)_4 \cdot 2H_2O$

Aysel Kanturk, Muge Sari, and Sabriye Piskin†

Department of Chemical Engineering, Yildiz Technical University, 34210, Istanbul, Turkey
(*Received 8 February 2007 • accepted 9 May 2008*)

Abstract−Sodium metaborate tetrahydrate ($NaB(OH)_4 \cdot 2H_2O$) was synthesized by reaction of anhydrous borax ($Na_2O \cdot 2B_2O_3$) with sodium hydroxide (NaOH) under conditions at 90 °C for 150 min. The structure was characterized by X-ray diffraction (XRD), Fourier transform infrared spectroscopy (FT-IR), Scanning electron microscope (SEM) and Thermogravimetric (TG) analyses. Moreover, dehydration kinetics of $NaB(OH)_4 \cdot 2H_2O$ was carried out under non-isothermal conditions and the Coats-Redfern method was applied to analyze the TG data for calculation of activation energies (E_a) and pre-exponential factors (k_o) for different heating rates. It was determined that dehydration of sodium metaborate tetrahydrate occurred in five steps. According to the Coats-Redfern non-isothermal model, E_a and k_o were calculated as 50.89 kJ/mol and 26×10^4 min^{-1} for region I, 18.51 kJ/mol and 0.87×10^3 min^{-1} for region II, 15.72 kJ/mol and 0.52×10^3 min^{-1} for region III, 4.37 kJ/mol and 0.04×10^3 min^{-1} for region IV and 37.42 kJ/mol and 8.56×10^3 min^{-1} for region V, respectively.

Key words: Sodium Metaborate, Sodium Borohydride, Synthesis, Crystal Structure, TG/DTG, Coats-Redfern

INTRODUCTION

The borates of sodium and their derivatives are the main materials for chemical and metallurgy industries and also the medical sector. Especially, sodium metaborate ($NaBO_2$) is commonly used in commercial production of sodium perborate tetrahydrate ($NaBO_2 \cdot H_2O_2 \cdot 3H_2O$), photographic and textile chemicals, detergents, cleaners and adhesives [1].

Turkey has 73% of the world's boron mineral reserves based on 851 million tons of B_2O_3 content. The most commercially important and frequently traded minerals are tincal ($Na_2B_4O_7 \cdot 10H_2O$), colemanite ($Ca_2B_6O_{11} \cdot 5H_2O$), ulexite ($NaCaB_5O_9 \cdot 8H_2O$) and kernite ($Na_2B_4O_7 \cdot 4H_2O$). These minerals can be refined into pure chemical compounds of commercial importance such as boric acid (H_3BO_3), anhydrous boric acid (B_2O_3), anhydrous borax ($Na_2B_4O_7$), borax pentahydrate ($Na_2B_4O_7 \cdot 10H_2O$), borax decahydrate ($Na_2B_4O_7 \cdot 5H_2O$). In addition, concentrated solution of $NaBO_2$ that is produced from borax by a reaction with caustic soda is directly reacted with hydrogen peroxide into produced $NaBO_2 \cdot H_2O_2 \cdot 3H_2O$ at the factories of Bandırma Eti Maden Works in Turkey [2].

$NaBO_2$ compounds can be classified according to water content inside as 4-hydrate, 2-hydrate and anhydrous. Sodium metaborate 4-hydrate transition to 2-hydrate is performed at lower temperature (53.5 °C) [3]. A temperature dependency of the $NaBO_2$ solubility can be determined by the equation [4]:

$$\text{Solubility of } NaBO_2 \text{ (g/100 g water)} = 245 + 0.915 \times T \text{ (K)} \quad (1)$$

Recently, $NaBO_2$ has very broad areas of R&D including hydrogen energy and its storage based on sodium borohydride ($NaBH_4$). Hydrogen technology is a key for a global energy system which is going to be independent of fossil fuels that cause global warming by the emissions of greenhouse gases such as CO_2, CH_4 and the other hydrocarbons. Hydrogen is a secondary energy that should be produced from primary and renewable energy sources such as wind, water, solar etc. and can be defined as an energy carrier [5,6]. Although hydrogen is the alternative energy for the future, there are some problems concerning its storage especially on-board to overcome. The use of traditional hydrogen storage technologies (such as high pressure, liquid state…) have been limited because of its danger, storage capacity and cost in storing and transporting. It has been suggested that $NaBH_4$ can be used as a hydrogen storage medium to overcome these problems [7,8].

When the production technologies of $NaBH_4$ are inspected, it is seen that there are some methods in which $NaBO_2$ is used as a starting material. Cooper et al. [9] reported the electrochemical conversion of $NaBO_2$ to $NaBH_4$ at room temperature. They concluded that borate ions from $NaBO_2$ can be reduced to borohydride ions in an electrolytic cell having a cationic-selective membrane separating the anode and cathode compartments and the overall reaction is given below:

$$NaBO_2 + 2H_2O \rightarrow NaBH_4 + 2O_2 \quad (2)$$

Kojima and Haga [10] concluded that $NaBH_4$ can be synthesized from $NaBO_2$ by annealing. The reaction of $NaBO_2$ and MgH_2 was carried out 550 °C under 7 MPa of hydrogen pressure for 2 h as given in Eq. (3).

$$NaBO_2 + 2MgH_2 \rightarrow NaBH_4 + 2MgO \quad (3)$$

The other reaction to synthesis of $NaBH_4$ using Mg_2Si and $NaBO_2$ is given in Eq. (4). The reaction of $NaBO_2$ and Mg mixed with Si was carried out at 400-550 °C under 7 MPa of H_2 pressure for 2 h [10].

$$NaBO_2 + Mg_2Si + 2H_2 \rightarrow NaBH_4 + 2MgO + Si \quad (4)$$

Li et al. [11] reported that borohydride can be obtained by a reaction of saline hydride with metaborate through ball milling at room temperature (Eq. (5), (6)). Even though the $NaBH_4$ conversion rate

†To whom correspondence should be addressed.
E-mail: piskin@yildiz.edu.tr

showed a deviation from its theoretical value, almost 100% of $NaBH_4$ conversion rate was achieved when an excessive amount of MgH_2 (1.25 times more than stoichiometric amount) was added.

$$2H_2 + 2Mg + NaBO_2 \rightarrow NaBH_4 + 2MgO \quad (5)$$

or

$$NaBO_2 + 2MgH_2 \rightarrow NaBH_4 + 2MgO \quad (6)$$

When the production technologies of $NaBH_4$ based on $NaBO_2$ are inspected, it is seen that $NaBO_2$ becomes quite essential in commercial borates class and hydrogen energy researches. The synthesis, crystal structure and dehydration kinetics analysis of $NaB(OH)_4 \cdot 2H_2O$, used as a starting material in production of $NaBH_4$, have become significant issues. Although there have been too many investigations of different types of boron minerals and products, there are only a few studies on synthesis and characterization of sodium metaborate hydrates.

Thermogravimetric analysis has been widely used to study the kinetics of thermal decomposition reactions of various materials such as polymer, coal, petroleum coke and mineral. Jun et al. [12] did a kinetic analysis of the thermal-oxidative decomposition of expandable polystyrene conventional by a thermogravimetric technique and calculated kinetic parameters by using differential and integrated methods. Park et al. [13] developed a kinetic analysis method by using a dynamic model that accounts for the thermal decomposition behavior of polymers with the variation of the conversion. It was found that the dynamic method gave a reliable value of kinetic parameters; and the activation energy and the reaction order of thermal decomposition of high-density polyethylene were larger than those of low-density and linear low-density polyethylene. Yoon et al. [14] studied the co-gasification of coal and petroleum coke by thermogravimetric analysis. Experiments were performed at various temperatures and the isothermal kinetics were analyzed and compared in the study.

The dehydration of hydrated boron minerals has been studied for a long time. Piskin [15] investigated the thermal properties of tincalconite, borax, kernite, probertite, ulexite, colemanite, hydroboracite, meyerhofferite, inyonite, kurnakovite, inderite, tunelite, howlite and veacite hydrate boron minerals. In the study, the change of crystal structure was also performed by IR spectrometry and x-ray diffraction analysis of the minerals. Sevim et al. [16] reported the kinetic analysis of thermal decomposition of boric acid by using thermogravimetric data. In this study, Suzuki and Coats-Redfern methods have been applied to the kinetic analysis. Erdogan et al. [17] examined the dehydration kinetics of howlite, ulexite and tunellite using thermogravimetric data.

The aim of this study is to synthesize of $NaB(OH)_4 \cdot 2H_2O$ and its structural characterization by X-ray diffraction (XRD), Fourier transform infrared spectroscopy (FT-IR), Scanning electron microscope (SEM) and Thermogravimetric (TG) analyses. In addition, the kinetic parameters of dehydration reactions of $NaB(OH)_4 \cdot 2H_2O$ were calculated by using TG data by the Coats-Redfern non-isothermal method.

EXPERIMENTAL

1. Synthesis of $NaB(OH)_4 \cdot 2H_2O$

Borax and sodium hydroxide were used as starting materials in our experimental studies. Borax with 99% purity, which contains 36.52% B_2O_3, 16.25% Na_2O and 47.23% H_2O, was provided from Bandırma Eti Mine Works and is abundantly found in Turkey.

The mixture of $Na_2B_4O_7$-NaOH (mole ratio, 1 : 2) and H_2O was packed into a stirred-type glass batch reactor which has an internal volume of 1 lt to synthesize sodium metaborate hydrate. The amount of water which was added to the mixture of starting materials was calculated according to the solubility data at reaction temperature (Eq. (1)). The reactor was heated at 90 °C for 150 minutes. During the reaction, it was observed that the color of the mixture changed from colorless to white. When the reaction was completed the saturated solution was filtered and cooled down to the room tempera-

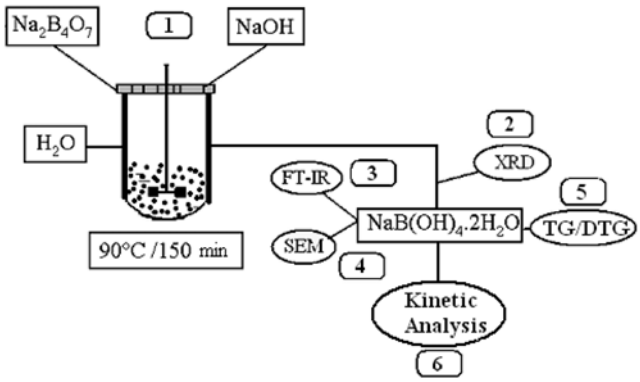

Fig. 1. Flow chart of investigation procedure.
(1) Synthesis of NaB $(OH)_4 \cdot 2H_2O$ by reaction of borax with sodium hydroxide under conditions at 90 °C and 150 min, (2) Crystalline structure analysis of $NaB(OH)_4 \cdot 2H_2O$, (3) Chemical structure analysis of $NaB(OH)_4 \cdot 2H_2O$, (4) Microstructure analysis of $NaB(OH)_4 \cdot 2H_2O$, (5) Thermal analysis of $NaB(OH)_4 \cdot 2H_2O$, (6) Dehydration kinetic analysis of $NaB(OH)_4 \cdot 2H_2O$ by Coats-Redfern method.

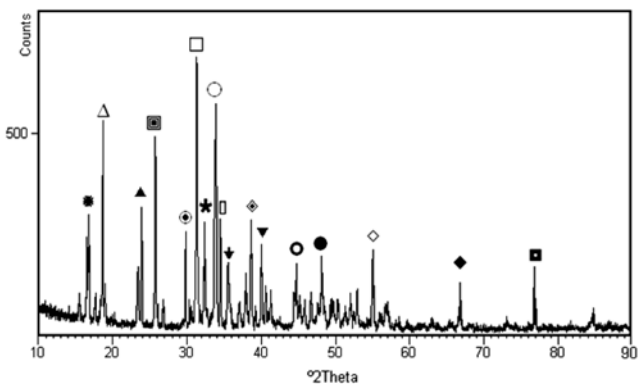

Fig. 2. X-Ray diffraction pattern of $NaB(OH)_4 \cdot 2H_2O$.
□: 31.32°-2.85619 Å-100%, ○: 33.88°-2.64600 Å-76.09%, △: 18.68°-4.75042 Å-73.08% ▣: 25.77°-3.45752 Å-71.05%, ▲: 23.89°-3.72536 Å-49.83%, ◈: 38.67°-2.32880 Å-41.14%, ✹: 16.81°-5.27367 Å-37.79%, ✱: 32.38°-2.76525 Å-34.78%, ▼: 40.00°-2.25406 Å-29.43%, ◇: 55.04°-1.66704 Å-29.10%, ⦿: 29.80°- 2.99781 Å-27.09%, ▯: 34.54°-2.59673 Å-26.42%, ⬇: 35.53°-2.52684 Å-26.09%, ●: 48.14°-1.89026 Å-23.75%, ◆: 66.77°-1.39984 Å-15.72%, ⭘: 44.76°-2.02468 Å-15.22%, ◘: 76.99°-1.24055 Å-10.20%

Table 1. Crystallographic parameters of $NaB(OH)_4 \cdot 2H_2O$

ICSD name	Sodium Borate Hydrate
ICSD reference code	01-076-0756
Empirical formula	BH_8NaO_6
Chemical formula	$NaB(OH)_4 \cdot 2H_2O$
Crystal system	Anorthic
Space groups	P-1
Space group number	2
Unit cell dimensions	a (Å): 6.1260, α (°): 67.9200
	b (Å): 8.1800, β (°): 110.5800
	c (Å): 6.0680, γ (°): 101.8500
Calculated density (g/cm^3)	1.74
Measured density (g/cm^3)	1.74
Volume of cell	262.85
Z, RIR	2.00, 0.48

ture. After cooling of the obtained saturated borate solution to room temperature, crystals were formed very easily. The flow chart of our investigation procedure is given in Fig. 1. According to the X-Ray analysis result, crystal structure was defined as sodium metaborate with 4 mole water and it is represented by the chemical formula of $NaB(OH)_4 \cdot 2H_2O$ (Fig. 2).

2. Crystalline Structure of $NaB(OH)_4 \cdot 2H_2O$

Crystalline structure of product was determined by wide-angle X-ray powder diffraction technique. Sample was ground in agate mortar and settled in an aluminum sample holder. Then the sample was compressed to have an even surface to prevent X-ray scattering. The X-ray analysis was carried out at an ambient temperature by using a Philips Panalytical X'Pert-Pro diffractometer in a range of diffraction angle from 10° to 90° with CuKα radiation (λ=0.15418 nm) at operating parameters of 40 mA and 45 kV with step size 0.02° and speed of 1°/min. Phase identification of sample was performed by inorganic crystal structure database (ICSD). The XRD pattern, and crystallographic parameters of $NaB(OH)_4 \cdot 2H_2O$ are given in Fig. 2 and Table 1, respectively.

3. Chemical Structure of $NaB(OH)_4 \cdot 2H_2O$

Attenuated total reflectance (ATR) of FT-IR spectroscopy (Perkin Elmer Spectrum One) was used in identification of chemical bonds of $NaB(OH)_4 \cdot 2H_2O$. Before the analysis, the crystal area had been cleaned and the background collected, the solid material was placed over the small crystal area on universal diamond ATR topplate. The FT-IR spectrum was achieved after force was applied to the sample, pushing it on to the diamond surface. The IR spectrum was recorded in the spectral range of 4000 to 650 cm^{-1} at ambient temperature and the resolution used was 8 cm^{-1}. FT-IR spectrum of $NaB(OH)_4 \cdot 2H_2O$ is given in Fig. 4.

4. Thermal Analysis of $NaB(OH)_4 \cdot 2H_2O$

Thermal dehydration of $NaB(OH)_4 \cdot 2H_2O$ was performed with Perkin Elmer Diamond TG\DTA instrument which was calibrated by means of the melting points of indium (T_m=156.6 °C) and tin (T_m=231.9 °C) under the same conditions with the sample. Samples were ground in agate mortar and stored under inert atmosphere before the analyses. Analyses were carried out at different heating rates of 2, 5 and 10 °C/min in an N_2 atmosphere which had a constant flow rate of 100 ml/min. The samples were settled in standard platinum crucibles and before use the crucible were washed with diluted HNO_3 solution in an ultrasonic bath during 30 minutes, then dried at 120 °C in an oven overnight. TG/DTG curves of $NaB(OH)_4 \cdot 2H_2O$ are shown in Fig. 5.

5. Dehydration Kinetic Analysis of $NaB(OH)_4 \cdot 2H_2O$

In the present study, the thermal dehydration reaction of $NaB(OH)_4 \cdot 2H_2O$ can be defined as below:

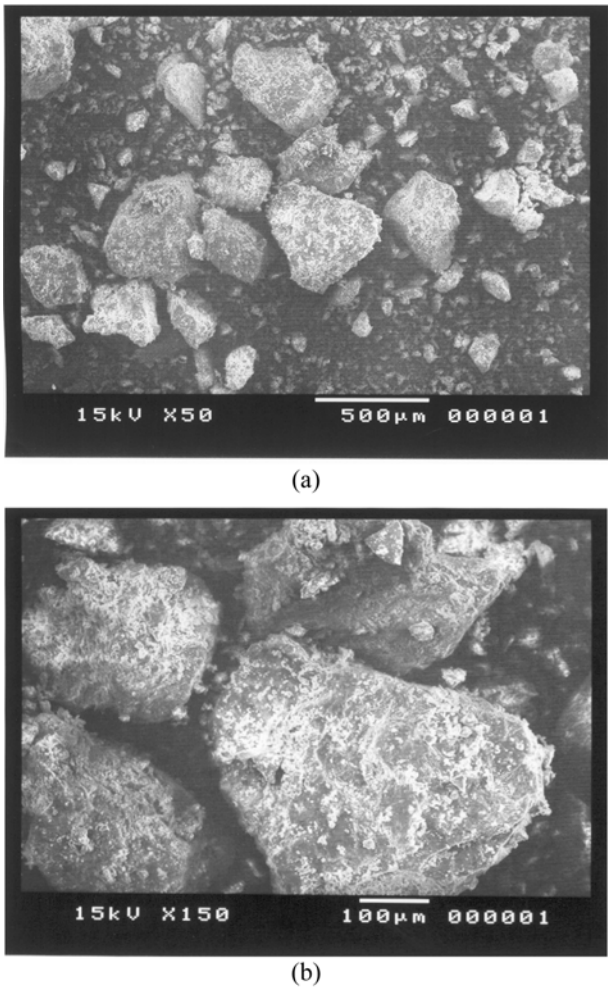

Fig. 3. The SEM images of $NaB(OH)_4 \cdot 2H_2O$ (a) ×50, (b) ×150.

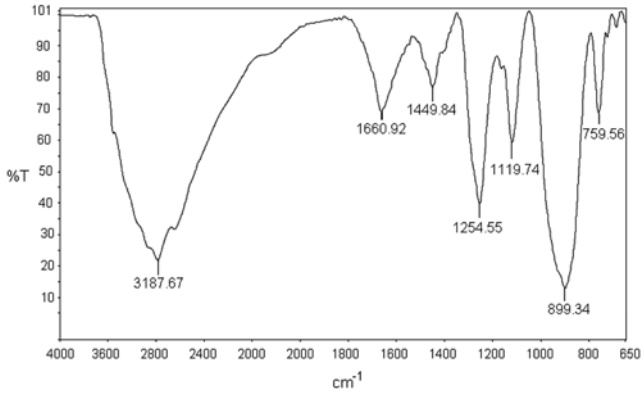

Fig. 4. The FT-IR spectrum of $NaB(OH)_4 \cdot 2H_2O$.

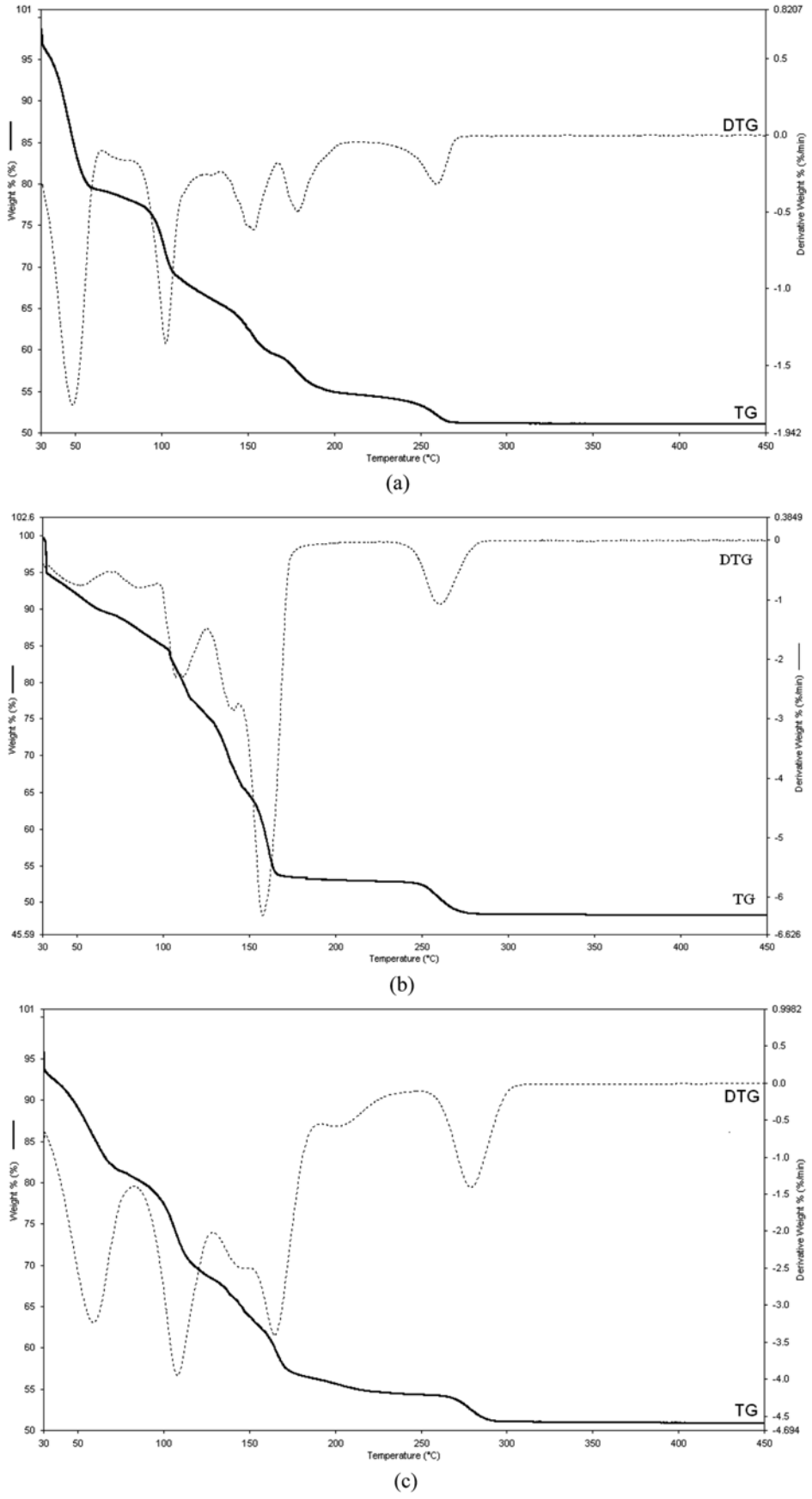

Fig. 5. TG/DTG curves of $NaB(OH)_4 \cdot 2H_2O$ obtained at different heating rates. The TG/DTG curves recorded under non-isothermal conditions in N_2 atmosphere: (a) 2 °C/min, (b) 5 °C/min and (c) 10 °C/min.

$$aA_{solid} \rightarrow bB_{solid} + cC_{gas} \quad (3)$$

Kinetic analysis of thermal dehydration of $NaB(OH)_4 \cdot 2H_2O$ was investigated by using the mathematical equation of the Coats-Redfern non-isothermal model based on TG data. According to the Coats-Redfern method, values of $[\log(-\log(1-\alpha)/T^2)]$ versus 1/T were plotted. The slope of the line was used to calculate E_a and also k_0 was determined from the intercept of the line. To calculate the kinetic parameters, the thermal dehydration reaction mechanism is assumed first order (n=1). The E_a and k_0 values at different heating rates are listed in Table 3.

$$\log\left[\frac{1-(1-\alpha)^{1-n}}{T^2(1-n)}\right] = \log\frac{k_0 R}{\beta E_a}\left[1-\frac{2RT}{E_a}\right] - \frac{E_a}{2.303RT} \quad \text{for } n \neq 1 \quad (4)$$

$$\log\left[\frac{-\log(1-\alpha)}{T^2}\right] = \log\frac{k_0 R}{\beta E_a}\left[1-\frac{2RT}{E}\right] - \frac{E_a}{2.303RT} \quad \text{for } n = 1 \quad (5)$$

RESULTS AND DISCUSSION

1. Crystal structure of $NaB(OH)_4 \cdot 2H_2O$

The crystal was found to be an anorthic crystal system with space group P-1. Crystallographic parameters and structure refinement are reported in Table 1. In the sample, peaks representative (2 0 0) and (−1 3 1) diffraction peaks corresponded to 31.32° and 33.88° diffraction angles, respectively, which characterized sodium metaborate tetrahydrate (Fig. 2). X-ray analysis of the product indicated that the 2.85619 Å peak at 31.32° had the maximum (100%) intensity compared with the reference $NaB(OH)_4 \cdot 2H_2O$ (references code: 01-076-0756) which is available in the ICSD database. XRD results prove that the produced crystals had the same crystal structure with $NaB(OH)_4 \cdot 2H_2O$.

The microstructure of the material was investigated by SEM (Jeol JSM-5410 LV) analysis. The sample was made ready for analysis by fixing to the device's sample holder with the help of a carbon sticky band. According to the SEM images, the particle size was approximately calculated as 444 μm (Fig. 3).

2. Chemical Structure of $NaB(OH)_4 \cdot 2H_2O$

The FTIR spectrum of this compound, which exhibited the following infrared absorption bands, is shown in Fig. 4. The band at 3186 cm^{-1} is the stretching mode of O-H. The band at 1661 cm^{-1} is assigned to the bending mode of H-O-H. The bands at 1450 and 899 cm^{-1} are assigned as the asymmetric and symmetric stretching of B-O, respectively. The band at 1255 cm^{-1} is assigned to the in-plane bending band of $(OH)^{-1}$. The band at 1120 is contributed with asymmetric stretching of B-O. The band at 760 cm^{-1} is assigned to the out-of-plane bending of $(OH)^-$ and symmetric stretching band of B-O [15].

According to crystal and chemical structure analysis results, the obtained product was best represented as $NaB(OH)_4 \cdot 2H_2O$ formula. All of the detected peaks in XRD pattern are indexed as those from 01-076-0756 powder diffraction file (PDF) which identify the $NaB(OH)_4 \cdot 2H_2O$. Also, the band at 1255 cm^{-1} in FT-IR spectrum is assigned to the in-plane bending mode of B-O-H which shows the compound contain $B(OH)_4^-$ ions. As a result, the sodium metaborate tetrahydrate product reaction can be defined as the following reaction:

$$1/4Na_2B_4O_7 + 1/2NaOH + 5/4H_2O \rightarrow NaB(OH)_4 \cdot 2H_2O \quad (5)$$

3. Thermal Analysis of $NaB(OH)_4 \cdot 2H_2O$

TG/DTG curves indicated that $NaB(OH)_4 \cdot 2H_2O$ underwent five basic dehydration steps at different heating rates. For a heating rate of 5 °C/min, the first two steps showed total weight loss of 24.37% that was observed in the temperature ranges 30.97-103.85 °C and 103.85-127.76 °C. It was attributed to the release of 1.86 moles of crystalline water and can be compared with the theoretical value of 2 for 5 °C/min. In the third step (127.76-148.76 °C), in fourth step (148.76-242.10 °C) and in fifth step (250.85-296.93 °C), weight losses of 0.79 mole, 0.88 mole and 0.30 mole were observed, respectively. This corresponds to the loss of 1.97 moles of structural water and can be compared with theoretical value of 2. Consequently, total weight loss was calculated as approximately 4 moles of water at 25-310 °C temperature range.

Table 2 shows the dehydration steps, weight losses and temperature ranges at 2, 5 and 10 °C/min heating rates. These overall de-

Table 2. Weight loss (%) and plots of kinetic equation calculated by Coats-Redfern method for all dehydration steps of $NaB(OH)_4 \cdot 2H_2O$ at 2, 5 and 10 °C/min heating rates

Heating rates (°C/min)	Reaction steps	DTG curve (°C)	Weight loss (%)	Plots equation	R^2
2	1.Step	31.40-90.25	20.13	y=−2999.2x+2.719	0.9784
	2.Step	90.29-121.01	10.08	y=−1055.7x−2.834	0.9742
	3.Step	121.06-168.41	7.89	y=−474.46x−4.336	0.9803
	4.Step	168.49-206.22	4.69	y=−570.39x−4.117	0.9721
	5.Step	206.29-283.38	3.55	y=−1319.7x−2.231	0.9893
5	1.Step	30.97-103.85	15.18	y=−2165.2x+0.601	0.9948
	2.Step	103.85-127.76	9.19	y=−918.32x−3.333	0.9803
	3.Step	127.76-148.76	10.40	y=−666.03x−3.9685	0.9897
	4.Step	148.76-242.10	11.62	y=−463.81x−4.4161	0.9749
	5.Step	250.85-296.93	4.00	y=−1074.1x−3.2231	0.9723
10	1.Step	30.68-84.47	13.34	y=−2657.9x+1.449	0.9784
	2.Step	84.47-132.94	12.64	y=−966.9x−3.246	0.9919
	3.Step	132.94-193.82	11.67	y=−820.94x−3.602	0.9971
	4.Step	193.82-245.84	1.64	y=−228.2x−4.919	0.9594
	5.Step	245.84-310.00	3.35	y=−1954.3x−1.658	0.9769

Table 3. Activation energies and pre-exponential factors at different heating rates for all dehydration steps of $NaB(OH)_4 \cdot 2H_2O$

Reaction steps	Heating rates (°C/min)					
	2		5		10	
	E_a (kJ/mol)	k_o (min^{-1})	E_a (kJ/mol)	k_o (min^{-1})	E_a (kJ/mol)	k_o (min^{-1})
1.step	57.43	20.95×10^4	41.46	45.48×10^3	50.89	26.00×10^4
2.Step	20.22	0.29×10^3	17.58	0.38×10^3	18.51	0.87×10^3
3.Step	9.09	0.03×10^3	12.75	0.15×10^3	15.72	0.52×10^3
4.Step	10.92	0.04×10^3	8.80	0.07×10^3	4.37	0.04×10^3
5.Step	25.27	0.65×10^3	20.57	0.49×10^3	37.42	8.58×10^3

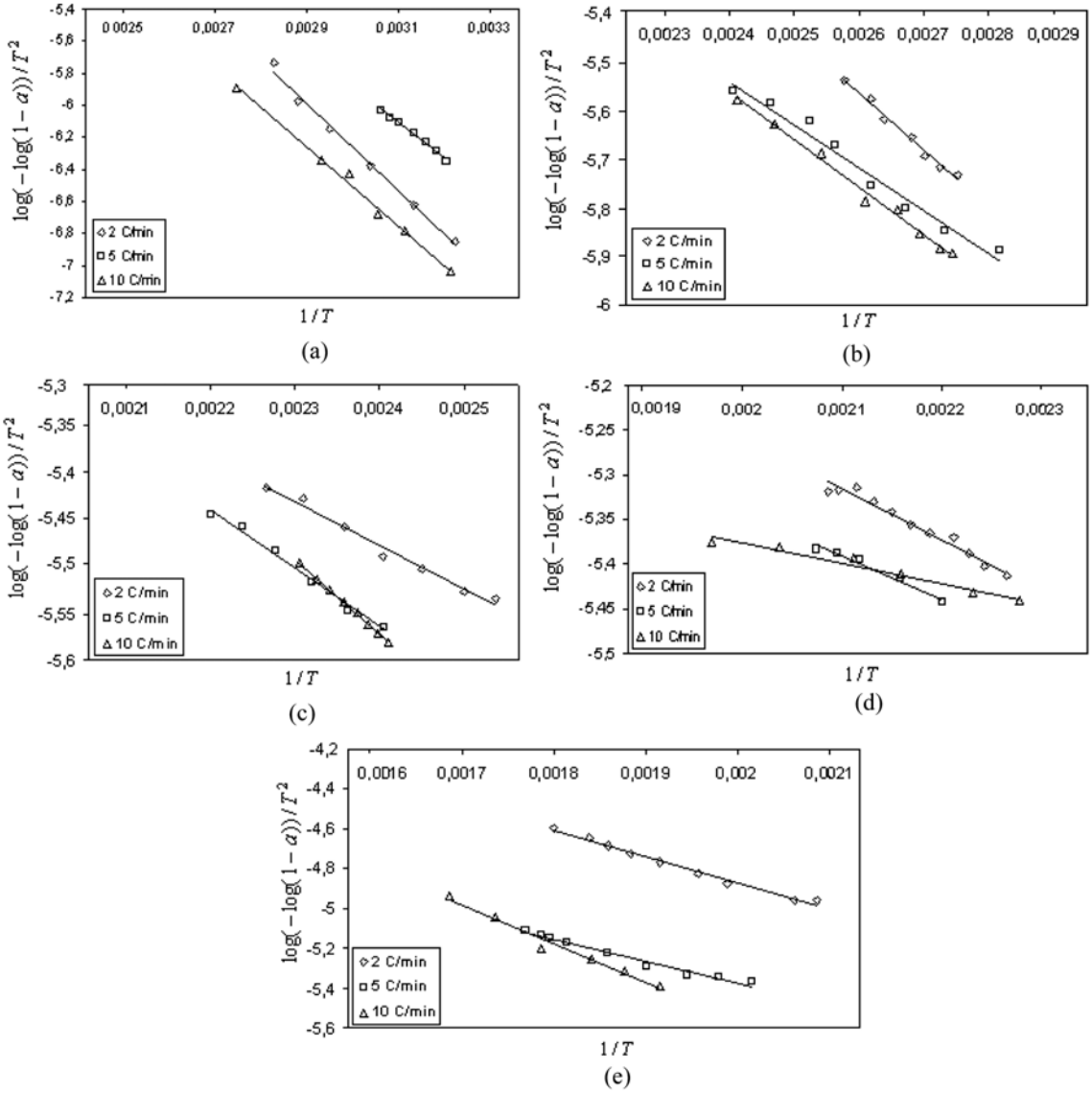

Fig. 6. Plots of kinetic calculated by Coats-Redfern method for all dehydration steps of $NaB(OH)_4 \cdot 2H_2O$ at 2, 5 and 10 °C/min heating rates: (a) 1.dehydration step, (b) 2.dehydration step, (c) 3.dehydration step, (d) 4.dehydration step and (e) 5.dehydration step.

hydration steps can be expressed as follows:

$$NaB(OH)_4 \cdot 2H_2O \rightarrow NaB(OH)_4 + 2H_2O \quad (6)$$

$$NaB(OH)_4 \rightarrow NaBO_2 + 2H_2O \quad (7)$$

4. Dehydration Kinetic Analysis

Decomposition fractions (α) of $NaB(OH)_4 \cdot 2H_2O$ in dehydration were determined according to TG curve and used in the calculation of kinetic parameters. The non-isothermal kinetic calculations were evaluated for all of the steps based on the Coats-Redfern equation

assuming first-order reaction. The values of E_a and k_0 were calculated from the slope and the intercept of the kinetic plots, respectively. The plots of the all dehydration steps are given in Fig. 6. It is noted that heating rate does not have a significant effect on the values of the activation energy (Table 3). According to the Coats-Redfern method, E_a and k_o were calculated for heating rate of 10 °C/min as 50.89 kJ/mol and 26×10^4 min^{-1} for region I, 18.51 kJ/mol and 0.87×10^3 min^{-1} for region II, 15.72 kJ/mol and 0.52×10^3 min^{-1} for region III, 4.36 kJ/mol and 0.04×10^3 min^{-1} for region IV and 37.42 kJ/mol and 8.56×10^3 min^{-1} for region V, respectively.

CONCLUSIONS

The present study investigated the synthesis, crystal structure and kinetic analysis of $NaB(OH)_4 \cdot 2H_2O$. The following key points can be made from this study:

1. We noticed that the main point of $NaB(OH)_4 \cdot 2H_2O$ production process is the determination of the amount of water which is added to the mixture of starting materials. In order to obtain saturated sodium borate solution at the end of the reaction, the amount of water should be calculated according to the solubility data.

2. The thermal dehydration of $NaB(OH)_4 \cdot 2H_2O$ occurs in five steps under nitrogen atmosphere. The first two steps are related to the release of crystalline water, and the last three steps are associated with loss of structural water. It was also determined that total weight loss of all steps was approximately 4 moles of water. Consequently, when results are compared with each other, they indicate that the total weight loss is independent of the heating rates.

3. Coats-Redfern method was used to estimate the kinetic parameters, assuming a first-order reaction. It is observed that calculated activation energies of the experiments performed at three different heating rates are acceptably close to each other for corresponding dehydration steps.

4. The production process including synthesis and dehydration steps can be expressed as the following reactions:

(1) $1/4\ Na_2B_4O_7+1/2\ NaOH+5/4H_2O \rightarrow NaB(OH)_4 \cdot 2H_2O$
(2) $NaB(OH)_4 \cdot 2H_2O \rightarrow NaB(OH)_4+2H_2O$
(3) $NaB(OH)_4 \rightarrow NaBO_2+2H_2O$

$NaBO_2$ which is prepared by the above reactions can be used where it is needed, especially as starting material for $NaBH_4$ production.

ACKNOWLEDGMENTS

The authors would like to gratefully acknowledge the financial support of The Prime Ministry State Planning Organization (Project No: 23-DPT-07-01-02).

NOMENCLATURE

T : temperature [K]
k_0 : pre-exponential factor [s^{-1}]
R : gas constant [8.314 $Jmol^{-1}K^{-1}$]
E_a : activation energy [$Jmol^{-1}$]
α : decomposition fraction [%]
β : heating rate [Ks^{-1}]

REFERENCES

1. E. D. Garret, *Borates, handbook of deposits, processing, properties and use*, Elsevier, 401 (1998).
2. The Report of Chemical Industry, Turkey State Planning Organization (2001).
3. D. L. Perry and S. L. Phillips, *Handbook of inorganic compounds*, CRC Press, New York (1995).
4. Y. Kojima, K. Suzuki, K. Fukumotoa, Y. Kawai, M. Kimbara, H. Nakanishi and S. Matsumoto, *J. Power Sources*, **125**, 22 (2004).
5. T. N. Veziroglu, *Int. J. Hydrogen Energ.*, **22**, 551 (1997).
6. I. Dincer, *Energy Policy*, **27**, 845 (1999).
7. H. I. Schlesinger, H. C. Brown, A. E. Finholt, J. R. Gilbreath, H. R. Hoekstra and E. K. Hyde, *J. Am. Chem. Soc.*, **75**, 215 (1953).
8. J. Kim, H. Lee, S. Han, H. Kim, M. Song and J. Lee, *Int. J. Hydrogen Energ*., **29**, 263 (2004).
9. B. H. H. Cooper, US Patent, 3,734,842 (1973).
10. Y. Kojima and T. Haga, *Int. J. Hydrogen Energ.*, **28**, 989 (2003).
11. Z. P. Li, N. Morigazaki, B. H. Liu and S. Suda, *J. Alloy Compd.*, **349**, 232 (2003).
12. H. Jun, S. C. Oh, H. P. Leeand and H. T. Kim, *Korean J. Chem. Eng.*, **23**, 761 (2006).
13. J. W. Park, S. C. Oh, H. P. Lee, H. T. Kim and K. O. Yoo, *Korean J. Chem. Eng.*, **17**, 489 (2000).
14. S. J. Yoon, Y. Choi, S. Lee and J. Lee, *Korean J. Chem. Eng*., **24**, 512 (2007).
15. S. Piskin, PhD Thesis, Istanbul Technical University, Faculty of Mining, Istanbul, Turkey (1983).
16. F. Sevim, F. Demir, M. Bilen and H. Okur, *Korean J. Chem. Eng*., **23**, 736 (2006).
17. Y. Erdogan, A. Zeybek, A. Sahin and A. Demirbas, *Thermochim. Acta*, **326**, 99 (1999).